Foam Drainage: Extended Large-Q Potts Model Simulation

Yi Jiang*, James A. Glazier
Department of Physics, University of Notre Dame, Notre Dame, IN 46556 USA

ABSTRACT

We study foam drainage using the large-Q Potts model extended to include gravity on a three dimensional lattice. Without adding liquid, homogeneously distributed liquid drains to the bottom of the foam until equilibrium between capillary effects and gravity is reached, while in an ordered dry foam, if a fixed amount of liquid is added from the top, a sharp flat interface between the wet and dry foam develops. The wetting front profile forms a downward moving pulse, with a constant velocity. The pulse decays over time while its leading edge for a brief time behaves like a solitary wave. With continuous liquid addition from the top, the pulse does not decay and we observe a soliton front moving with a constant velocity. Continuously adding liquid to an initially wet foam keeps the liquid profile constant. Our simulations agree with both experimental data and simplified mean field analytical results for ordered foams but predict an unstable interface for disordered foams.

INTRODUCTION

Foams are macroscopically structured cellular materials, of practical importance in applications from brewing to lubrication. A liquid foam, with clearly separated liquid and gas phases, has a characteristic time scale of evolution and distinct rheological properties [1]. Foams are also a model for other nonequilibrium, disordered materials, such as polycrystalline metals, in which the dynamics is driven by the surface energy. Characterizing the structure and evolution of foams challenges current theory and experiments. In three dimensional liquid foams, gravitational drainage of the liquid is an additional complication. Often drainage, rather than diffusion, determines foam stability and properties. Mysels *et al.* were the first to investigate the different types of thin film drainage [2], concentrating on vertical films formed by withdrawing glass frames from pools of surfactant solution. Early experiments, measuring the amount of drained liquid as a function of time, did not offer much immediate insight [3]. Princen [4] has discussed the asymptotic vertical equilibrium profile of drainage by considering the osmotic pressure of foams. Mean field calculations on the microflow in Plateau channels in relatively dry foams suggested a solitary wave solution for liquid flow in foam [5] [6]. Recently Weaire *et al.* measured the velocity of the interface between the dry and wet monodisperse foams in terms of the rate of continuous addition of liquid from the top. AC capacitance and conductance measurements of the vertical liquid profiles for different types of drainage could not distinguish horizontal wetness changes [7] [8] [9]. Because the foam is inhomogeneous and resembles a porous medium, we might expect that the penetration of liquid into the Plateau channels would result in an unstable interface or in viscous fingering. Instead, the mean field theory predicts a flat interface.

Magnetic resonance imaging (MRI) allows a non-invasive visualization of the interior structure of foams. German, McCarthy *et al.* measured one dimensional vertical wetness profiles of draining beer foams, whipped cream, and egg white *etc.* [10]. Prause *et al.* have taken images of three dimensional foams with high resolution [12] and 1-d drainage profiles,

but the full three dimensional drainage experiments remain to be done.

MEAN FIELD CALCULATIONS

Theoretical calculations of the liquid flow during foam drainage assume that the liquid flows through a system of interconnected, randomly oriented Plateau channels, with negligible flow through the much thinner soap films [2]. A monomolecular layer of surfactant on the film surfaces reduces the surface tension and retards liquid flow, resulting in non-slip conditions on the boundaries of channels. Neglecting bubble size distribution, bubble density and liquid viscosity *etc.* produces a mean field theory.

The capillary pressure, i.e. the pressure across the liquid surface, is: $P_{capillary} = P_l - P_g = \frac{2\gamma\cos\theta}{r}$, where γ is the surface tension, θ is the contact angle between liquid and gas, and P_l and P_g are the pressure of the liquid and gas, respectively.

For an incompressible liquid, the derivative of equation (1) yields the between the change of gas pressure δP and the change in the channel area δs:

$$\delta P = \gamma\alpha s^{-3/2}\delta s, \tag{1}$$

where α is a constant determined by the curvature of the lateral surface of the channel. For ideal Plateau channels, the radius of curvature of the lateral surface r can be related to the area of the Plateau channel s by $s = (\sqrt{3} - \pi/2)r^2$, yielding $\alpha = (\sqrt{3} - \pi/2)^{\frac{1}{2}}$.

Assuming the motion of the liquid in Plateau channels to be microscale flow, we apply the continuity equation to the channel flow:

$$\frac{\partial s}{\partial t} + u\frac{\partial s}{\partial x} + x\frac{\partial u}{\partial x} = 0, \tag{2}$$

where u is the velocity of the flow.

Following the derivation in [5], we consider the solution of the Navier-Stokes equation for massive fluid in a tube of arbitrary cross section:

$$u = -\frac{s}{\beta\eta}\left[\frac{1}{3}\frac{\partial P}{\partial x} - \rho g\right], \tag{3}$$

where η is the viscosity of the fluid, the factor $1/3$ comes from averaging over the directions of motion of the liquid, and β is a numerical coefficient depending only on the shape of the cross section of the channel: e.g. $\beta = 8\pi$ for a tube of circular section, $\beta = 49.1$ for a cross section in the form of a Plateau triangle [5]. This equation can also be viewed as the force balance between the capillary force, the pressure gradient and gravity [6].

If we eliminate p and u from the above equations and introduce $x_0 = \sqrt{\gamma/\rho g}$ and $t_0 = \beta\eta/\sqrt{\gamma\rho g}$, the equations are reduced to a nonlinear PDE:

$$\frac{\partial S}{\partial \tau} - \frac{\partial}{\partial X}\left[\alpha S^{1/2}\frac{\partial S}{\partial X} - S^2\right] = 0, \tag{4}$$

with dimensionless variables $X = x/x_0$, $\tau = t/t_0$ and $S = s/{x_0}^2$.

Solving equation(4) in a moving frame, we get the following three solutions:

$$S = \begin{cases} v \\ v\tanh^2\left[\frac{\sqrt{v}}{\beta}(X - v\tau)\right] \\ v\coth^2\left[\frac{\sqrt{v}}{\beta}(X - v\tau)\right] \end{cases}. \tag{5}$$

The first solution to the channel area describes a steady state, in which the drainage reaches an equilibrium with the influx of liquid. The second solution is not physical as it diverges at $X - v\tau = 0$. The last one, a solitary wave traveling at a constant velocity, was observed in experiments and was proposed in [5] and [6].

SIMULATIONS

The large-Q Potts model partitions the foam on a three dimensional square lattice. A bubble, σ, is the collection of lattice sites $\vec{i} = (x, y, z)$ with spin $\sigma(\vec{i}) = \sigma$, σ ranging from 1 to Q ($Q > 5000$ in this study). While it was originally used to simulate foam coarsening [13] in static one-phase systems, it can be easily extended to include drainage. We treat the two phases in the system, liquid and gas, as two bubble types, with the liquid represented as a single bubble subject to a gravitational field. The extended Potts Hamiltonian of the system is then:

$$\mathcal{H}_{Potts} = \sum_{\vec{i},\vec{i}' neighbors} J_{\tau(\sigma),\tau(\sigma')}[1 - \delta_{\sigma(\vec{i}),\sigma(\vec{i}')}] + \sum_{liquid} g\ x_{liquid}. \tag{6}$$

where $J_{\tau(\sigma),\tau(\sigma')}$ is the coupling constant between bubbles, where $J_{gas,gas} > J_{gas,liquid} > J_{liquid,liquid}$; g is the force of gravity per unit density and x_{liquid} is the average height of the liquid component of the foam. The second term in $\mathcal{H}_{Potts}$ applies to liquid only.

At each time step, a site is selected at random, and a spin change to a neighboring spin proposed. Only the changes that lower the total energy of the system are accepted, corresponding to zero temperature dynamics.

Boundary conditions are periodic in the horizontal direction but rigid in the vertical direction. We use a very ordered initial foam which affects the shape of the wetting interface. We monitor the mean liquid fraction as a function of vertical position. Free drainage has no input of liquid and the liquid begins with a homogeneous vertical distribution. In pulsed drainage, the foam is initially dry and a fixed amount of liquid placed above the dry foam drains under gravity. In forced drainage, liquid is added from the top of the foam at a constant rate, different initial conditions (wet or dry foams) resulting in different profiles.

DISCUSSION

Figure 1a shows the time evolution of the liquid profiles in free drainage. With no liquid input, the initially homogeneously distributed liquid drains downwards until gravity is balanced by capillary effects, to produce an equilibrium profile. Drainage profiles from MRI experiments by McCarthy [10] and our group(figure 1b) are very similar, though it is difficult to compare them quantitatively. Efforts to quantify the slope of the linear part of the profile have not had much success.

In figure 2, we plot the liquid profiles for pulsed drainage. The pulse is monitored as it descends. The leading edge of the pulse, over short intervals such that decays is negligible, is quantitatively identical to the soliton in [9] [8]. In figure 2, we fit the leading edges of profiles to the same soliton solution. A longer time simulation (long distance for the pulse) allows us to see liquid transfer from the peak of the soliton to the tail, resulting in pulse spreading. The wave front of the soliton moves at a constant velocity, in good agreement with [9]. The high frequency structure of the solitary wave is due to the ordered structure of the simulated foams, shown in the vertical cross sections in figure 3.

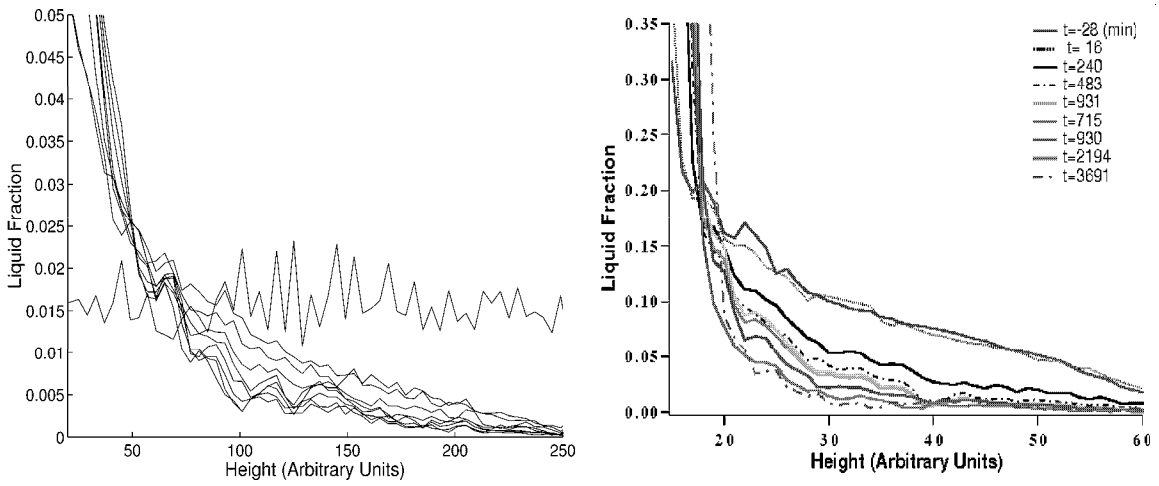

(a) Potts Model Simulation (b) MRI experimental data

Figure 1. Liquid profiles for gravitational drainage as a function of time

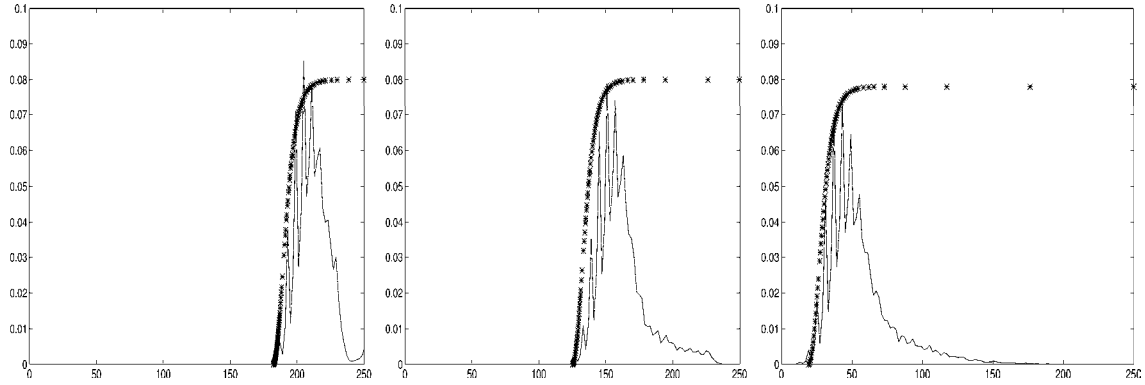

(a) 3000 (b) 5000 (c) 9000

Figure 2. Liquid profiles for pulsed drainage in Monte Carlo steps (MCS)

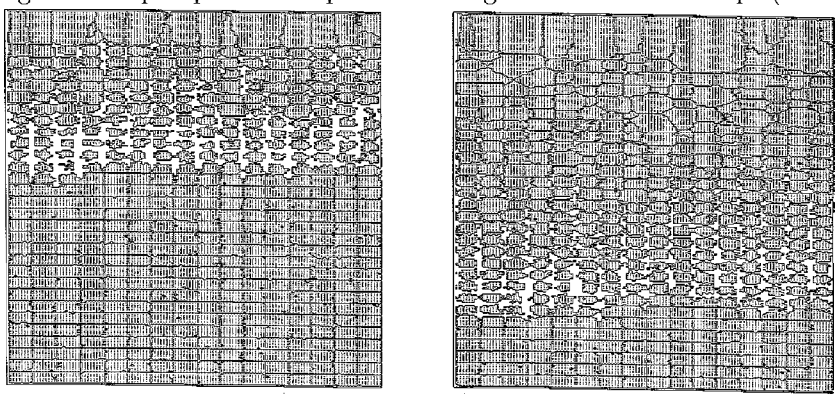

(a) 3000 MCS (b) 8000MCS

Figure 3. Snapshots of vertical cross sections of pulsed drainage

Naturally, for a continuous liquid supply, the soliton has a non-decaying fixed profile (Figure 4a), matching both the analytic solution and the experiment results. In addition, the width of the wave front spreads over time, as predicted in [7].

On the other hand, if the foam is initally wet, continuously adding liquid does not change the shape of the profiles except to increase the foam wetness (Figure 4b), indicating equilibrium between the liquid input, gravity and capillary forces, corresponding to the steady state solution $S = v = constant$.

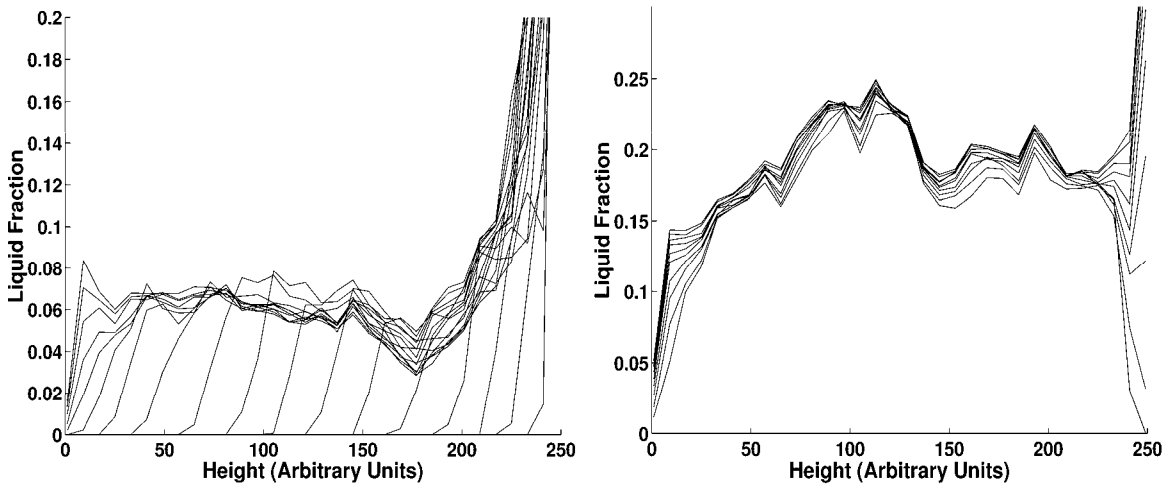

(a) Initially dry foam (b) Initially wet foam

Figure 4. Liquid profiles for forced drainage

When the rate of coarsening is comparable to that of drainage, the interface between the wet and dry foam is diffuse due to the disordered structure. The liquid forms clusters in the middle of the foam (Figure 5). The penetrating of liquid into relatively dry foam through the Plateau channels resembles the front instability of viscous fingering. Thus mean field theory fails for disordered foams. When drainage is much faster than coarsening, the interface is flat, within a band thinner than the dimension of a bubble. Thus drainage of a disordered foam is actually a porous medium problem with evolving pore sizes and shapes.

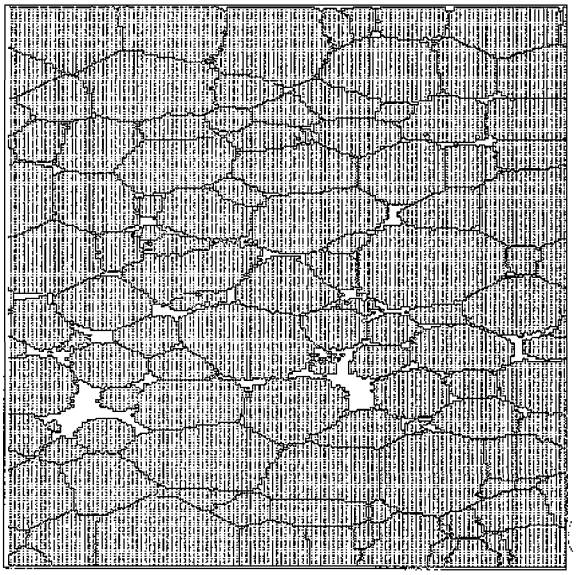

Figure 5. Snap shot of drainage in a disordered foam.

CONCLUSIONS

The extended large-Q Potts model simulations produce results comparable to experiments and also validate the mean field drainage theory for ordered foams. The model allows us to continuously vary the liquid content, as well as the strength and range of interactions between like and unlike phases. With experimental data for foams of varying compositions and growth characteristics, we will develop our simulation to predict the behavior of foams of arbitrary viscosity and wetness, leading to quantitative simulations of the properties of

industrial foams.

ACKNOWLEDGMENTS

The authors acknowledge support from the Exxon Educational Foundation, ACS/PRF & NSF/NYI DMR-9257011.

REFERENCES

---

* Electronic address: yjiang@charpentier.phys.nd.edu

[1] A. Kraynik, Ann. Rev. Fluid Mech., **20**, 325 (1988).
[2] K. J. Mysels, K. Shinoda, S. Frankel, *Soap Films: Studies of Their Thinning and a Bibliography*, Pergamon Press, Oxford (1959).
[3] J. J. Bikerman, *Foams: Theory and Industrial Applications*, Reinhold, New York, (1953).
[4] H. M. Princen, Langmuir **2**, 518 (1986).
[5] I. I. Gol'dfarb, K. B. Kann, and I. R . Sreiber, Fluid Dyn. **23**, 244 (1988) and references therein.
[6] G. Verbist and D. Weaire, Euro. Phys. Lett. **26**,631 (1994).
[7] D. Weaire, N. Pittet, S. Hutzler and D. Pardal, Phys. Rev. Lett. **71** 2670 (1993).
[8] D. Weaire, S. Findlay and G. Verbist, J. Phys. Condens. Matter **7**, L217 (1995).
[9] S. Hutzler, G. Verbist, D. Weaire and K. A. van der Steen, Europhys. Lett. **31**, 497 (1995).
[10] J. B. German and M. J. McCarthy, J. Agric. Food Chem. **37**, 1321 (1989); M. J. McCarthy and E. Perez, Biotechnol. Prog. **7** 540 (1991).
[11] C. P. Gonatas, J. S. Leigh, A. G. Yodh, J. A. Glazier and B. Prause, Phys. Rev. Lett. **75**, 573 (1995).
[12] B. A. Prause, J. A. Glazier, S. J. Gravina and C. D. Montemagno, J. Phys. Condens. Matter **7**, L511 (1995).
[13] M. P. Anderson, D. J. Srolovitz, G. S. Grest and P. S. Sahni, Acta metal. **32**, 783 (1984) J. A. Glazier, M. P. Anderson, and G. S. Grest, Philos. Mag. B **62**, 615 (1990).
[14] J. A. Glazier, Ph.D. thesis, Univ. of Chicago (1989) unpublished.
[15] J. Stavans and J. A. Glazier, Phys. Rev. Lett.**62**, 1318 (1989); J. A. Glazier, S. P. Gross, and J. Stavans, Phys. Rev. A **36**, 306 (1987).